Intrinsic concentration, effective densities of states, and effective mass in silicon

Martin A. Green
Joint Microelectronics Research Centre, University of New South Wales, Kensington, Australia 2033

(Received 29 August 1989; accepted for publication 14 November 1989)

An inconsistency between commonly used values of the silicon intrinsic carrier concentration, the effective densities of states in the conduction and valence bands, and the silicon band gap is resolved by critically assessing the relevant literature. As a result of this assessment, experimentally based values for the valence-band "densities-of-states" effective mass are determined in the 300–500 K range and are shown to be in good agreement with recent theoretical calculations. At 300 K, experimentally based values of 3.1×10^{19} cm^{-3} for the valence-band effective densities of states and 1.08×10^{10} cm^{-3} for the intrinsic carrier concentration are determined. Although in good agreement with theoretical calculations, these are significantly higher and lower, respectively, than commonly used values in the past. These results have important implications in the calculation of other silicon material and device parameters.

I. INTRODUCTION

A parameter of prime importance in semiconductor device physics is the intrinsic carrier concentration.[1] The effective densities of states in the conduction and valence bands play a similarly important role.[1] The latter also are important more generally in semiconductor physics, for example, in the interpretation and modeling of the properties of levels introduced by dopants, impurities, and defects into the semiconductor forbidden gap.[2] The carrier effective masses are accessible experimentally and enter into the theoretical expressions for the previous parameters as well as into the expressions for the carrier thermal velocities. The latter are again important in the interpretation and modeling of the properties of gap levels.[2]

Despite the importance of these parameters, commonly used values (e.g., Refs. 1, 3, and 4) are easily shown to form inconsistent sets. The magnitude of this inconsistency is such that, in energy determinations, errors of up to 30 meV can result as can errors in carrier concentrations and device terminal properties of a factor of 2. Significant errors can also occur in calculating impurity ionization percentages and optical and electronic capture cross sections of dopant and defect levels.

The aim of the present work is to identify the source of the inconsistency mentioned above by critically evaluating the literature leading to the adoption of currently accepted values. As a result of this examination, a self-consistent set of these parameters was identified that removes the discrepancies previously noted.

As an additional result of this work, experimentally based values for the valence-band density of states and the corresponding valence-band effective mass are derived over the 300–500 K range.

II. CALCULATED VALUES

The intrinsic concentration n_i and the effective densities of states in the conduction and valence bands, N_C and N_V, respectively, are related by the semiconductor band gap E_g

$$n_i^2 = N_C N_V \exp(-E_g/kT), \tag{1}$$

where k is Boltzmann's constant and T the absolute temperature. N_C and N_V are given by[1]

$$N_C = 2(2\pi m_{dc}^* kT/h^2)^{3/2}, \tag{2}$$

$$N_V = 2(2\pi m_{dv}^* kT/h^2)^{3/2}, \tag{3}$$

where m_{dc}^* and m_{dv}^* are the density-of-states effective masses in the conduction and valence bands, respectively, and h is Planck's constant. Replacing physical constants by their recommended values[5] gives

$$N_C = 2.540\,933(32)\times10^{19}(m_{dc}^*/m_0)^{3/2}(T/300)^{3/2}\text{cm}^{-3}, \tag{4}$$

$$N_V = 2.540\,933(32)\times10^{19}(m_{dv}^*/m_0)^{3/2}(T/300)^{3/2}\text{cm}^{-3}, \tag{5}$$

where m_0 is the electron rest mass and the digits in parentheses following 2.540 933 indicate the uncertainty in the preceding digits. (This is a convention which will be adopted throughout this paper.) Explicit values for N_C and N_V can be calculated once the effective masses are known (generally temperature dependent).

Silicon has six equivalent conduction-band minima forming ellipsoidal constant energy surfaces located about 85% of the distance along (100) equivalent directions in phase space towards the edge of the first Brillouin zone.[6] The corresponding density-of-states effective mass is

$$m_{dc}^* = 6^{2/3}(m_t^{*2}\, m_l^*)^{1/3}, \tag{6}$$

where m_t^* and m_l^* are the transverse and longitudinal effective masses associated with the ellipsoidal constant energy surfaces. The structure near the valence-band maximum at the center of the Brillouin zone consists of doubly degenerate "light" and "heavy" hole bands plus a "split-off" hole band. Assuming these bands are isotropic and parabolic, the valence-band density-of-states effective mass is given by

$$m_{dv}^* = \{m_{lh}^{*3/2} + m_{hh}^{*3/2} + [m_{so}^* \exp(-\Delta/kT)]^{3/2}\}^{2/3}, \tag{7}$$

where m_{lh}^*, m_{hh}^*, and m_{so}^* are the effective masses of the bands suggested by the respective subscripts and Δ is the energy

 0021-8979/90/062944-11$03.00

difference between the energy maximum in the "split-off" band and the other two bands. Its measured value is 0.0441(3) eV at 1.8 K.[7]

Low-temperature cyclotron resonance studies give[8]

$$m_t^* = 0.1905(1)m_0, \tag{8}$$

$$m_l^* = 0.9163(4)m_0. \tag{9}$$

Note that the above value of m_l^* differs significantly from the often quoted larger value of 0.98.[1,9] The larger value actually arises from the earliest cyclotron resonance measurements of these parameters.[10,11] Several more recent studies confirm the smaller value[12,13] which can now be in little doubt.

In an earlier review of the topic of the present paper, Barber[6] suggested a temperature dependence of conduction-band effective mass based on the good agreement between cyclotron resonance measurements of Stradling and Zhukov[14] at low temperatures and Faraday effect measurements of Ukhanov and Mal'tsev[15] at higher temperatures. However, subsequent and more accurate cyclotron resonance measurements of the transverse effective mass[16] have suggested a much lower temperature dependence than these earlier measurements. A closer examination of the results of Ukhanov and Mal'tsev[15] also shows that the postulation of a relatively large effective mass increase with temperature is based on an anomalously high 23% increase in electron concentration in a phosphorus-doped silicon specimen when heated from 293–600 K. This anomaly was attributed to "the impurity levels of phosphorus atoms." A more likely explanation would be the temperature dependence of the Hall factor for electrons[17]; a parameter assumed constant in calculating the previous results. As a consequence, there is now no soundly based experimental support for the temperature dependence of the conduction-band effective mass proposed by Barber.[6]

The most reliable measurements to date of the temperature dependence of the transverse effective mass are those of Ousset *et al.*[16] These results are included in Fig. 1. There are theoretical grounds for expecting an even weaker dependence of the longitudinal effective mass.[14] The experimental results of Stradling and Zhukov[14] support this view, although some doubt is cast on this result by the corresponding overestimation of the temperature dependence of the transverse mass.

Theoretically, a change in conduction-band effective mass with temperature could be expected from two effects: (1) a change in the shape of the energy-momentum curves with temperature as the lattice expands and more significantly as electron-phonon interaction energies change[18]; (2) increasing occupation of the regions of the band away from the band edge at increased temperature, which will highlight any departures from parabolicity expected in these regions.

Macfarlane *et al.*[19] suggest a very simple model for the former effect of temperature. The model assumes that the decrease with temperature observed for the silicon band gap is simply due to a temperature-dependent energy scaling factor. As the temperature increases, states away from the band edge would then approach the other band more quickly than those at the edge. This would flatten the bands and so increase effective masses. Results from recent theoretical studies of the temperature dependence of the silicon band energies[18] show some correlation between the energy above the valence-band maximum of the limited fraction of conduction-band states studied and the reduction of this energy with temperature. Such a model would predict an effective mass increasing with temperature by a factor $E_{G0}/E_G(T)$, where E_{G0} is the value of the band gap $E_G(T)$ at $T = 0$ K. This is presumably the origin of such an "energy dispersion" factor which appears in the work of Barber.[6]

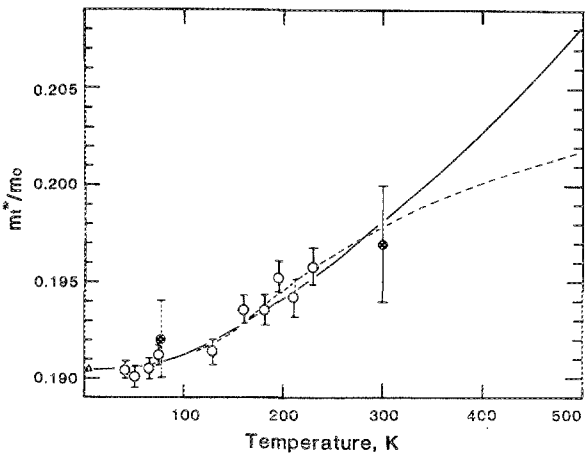

FIG. 1. Experimental transverse effective mass in silicon (m_t^*/m_0) as a function of temperature (Refs. 8 and 16). The solid line shows the function [$0.1905\,E_{G0}/E_G(T)$] found to describe the data from 0–300 K. The dotted line shows a more conservative extrapolation of the data giving a 3.5% lower estimate of m_t^* at 500 K.

Rather surprisingly, it was noted in the present work that the experimental temperature dependence of m_t^* shown in Fig. 1 could be described to within experimental accuracy by multiplying the measured low-temperature value by this factor. This provides a useful parametrization of these data, although the explanation for the good fit may be more subtle than that outlined above. Ousset *et al.*[16] have interpreted the temperature dependence of the same data in terms of a nonparabolicity of the conduction bands. Other experimental and theoretical work supports this interpretation.[16]

In summary, recent experimental work suggests a relatively weak temperature dependence of m_t^* and theoretical considerations suggest an even weaker dependence of m_l^*. The approach used in the calculations that follow will be to assume m_l^* has the value $0.9163m_0$, independent of temperature, and to assign m_t^*/m_0 the value $0.1905E_{G0}/E_G(T)$ (expressions for $E_G(T)$ are subsequently discussed]. Using this formulation, the low-temperature density-of-states effective mass would be $1.062m_0$ at 4.2 K in agreement with Barber.[6] However, the best present estimate of the 300-K value of m_{dc}^* would be $1.09\,m_0$, somewhat lower than the value of $1.18\,m_0$ suggested by Barber.[6] The best present estimate of the variation of m_{dc}^* with temperature is included in Table I, discussed subsequently. The values shown are reasonably soundly based for temperatures below 300 K, but are less soundly based above this temperature. However, due to the small variation with temperature expected from both theoretical and experimental considerations, the tabulated val-

TABLE I. Calculated dependence upon absolute temperature of the silicon intrinsic carrier concentration, n_i, the effective densities of states, N_C and N_V, the density-of-states effective masses, m^*_{dc} and m^*_{dv}, and the thermal velocity effective masses, m^*_{tc} and m^*_{tv}. Also shown is the band gap, E_G, based on the best available experimental data (Refs. 19 and 35).

T (K)	n_i (cm^{-3})	N_C (cm^{-3})	N_V (cm^{-3})	E_G (eV)	m^*_{dc}/m_0	m^*_{dc}/m_0	m^*_{tc}/m_0	m^*_{tv}/m_0
4.2	3.14×10^{-686}	4.55×10^{16}	1.87×10^{16}	1.1700	1.06	0.59	0.27	0.37
50	1.64×10^{-41}	1.87×10^{18}	9.78×10^{17}	1.1690	1.06	0.69	0.27	0.39
100	1.95×10^{-11}	5.31×10^{18}	3.66×10^{18}	1.1649	1.06	0.83	0.27	0.41
150	3.16×10^{-1}	9.81×10^{18}	8.16×10^{18}	1.1579	1.07	0.95	0.27	0.42
200	5.03×10^{4}	1.52×10^{19}	1.43×10^{19}	1.1483	1.08	1.03	0.27	0.41
250	7.59×10^{7}	2.15×10^{19}	2.20×10^{19}	1.1367	1.08	1.10	0.27	0.41
300	1.07×10^{10}	2.86×10^{19}	3.10×10^{19}	1.1242	1.09	1.15	0.28	0.41
350	3.92×10^{11}	3.65×10^{19}	4.13×10^{19}	1.1104	1.10	1.19	0.28	0.40
400	6.00×10^{12}	4.51×10^{19}	5.26×10^{19}	1.0968	1.11	1.23	0.28	0.40
450	5.11×10^{13}	5.43×10^{19}	6.49×10^{19}	1.0832	1.12	1.29	0.28	0.40
500	2.89×10^{14}	6.46×10^{19}	7.81×10^{19}	1.0695	1.13	1.29	0.28	0.39

ues are expected to be accurate to within a few percent over the temperature range shown.

Another important effective mass is that which determines the average thermal velocity of carriers v_{th} as described by the expression

$$v_{th} = (8kT/\pi m^*_{th})^{1/2}. \quad (10)$$

For the conduction band, this thermal velocity effective mass, m^*_{tc}, is given by[20]

$$m^*_{tc} = 4m^*_l/[1 + (m^*_l/m^*_t)^{1/2} \sin^{-1}(\delta)/\delta]^2, \quad (11)$$

where

$$\delta^2 = (m^*_l - m^*_t)/m^*_l. \quad (12)$$

Using the same values of m^*_l and m^*_t as for the density-of-states calculation, the calculated temperature variation of the thermal velocity effective mass is also included in Table I. This mass is required for calculating cross sections from capture rates.

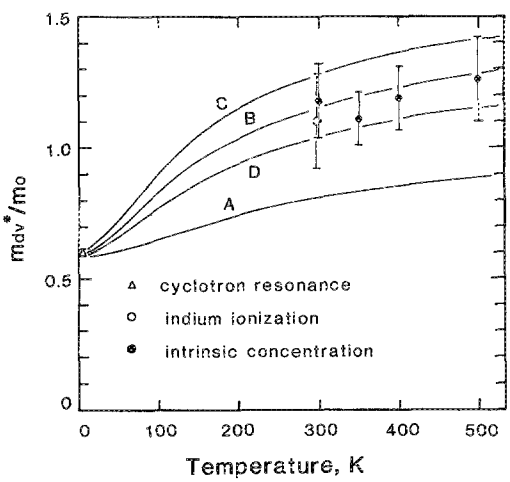

FIG. 2. Valence-band density-of-states effective mass in silicon (m^*_{dv}/m_0) as a function of temperature. Curves A (Ref. 6), B (Ref. 24), C (Ref. 20), and D (Ref. 20), show the results of theoretical calculations based on low-temperature cyclotron resonance data (Ref. 21). The high-temperature experimental points are derived in the present work from indium ionization data (Ref. 26) and from experimental measurements of the intrinsic carrier concentration. The error bars show the one-standard-deviation uncertainty in the experimental data.

In contrast to the conduction-band effective mass, that for the valence band is expected to be more temperature sensitive. Not only is there an explicit temperature dependence as indicated by Eq. (7) due to increasing hole population in the split-off band at high temperatures, but all three bands are known to be nonisotropic and nonparabolic. Band parameters have been extracted from the experimental cyclotron resonance studies of Hensel and Feher[21] by Balslev and Lawaetz,[22] Lawaetz,[23] and in an unpublished work of Hensel cited by Humphreys.[20]

Recent theoretical calculations of Madarasz *et al.*[24] and Humphreys[20] show that the earlier work of Barber[6] underestimated the temperature dependence arising from the anisotropy and nonparabolicity of these bands. Figure 2 compares the results of these calculations. Curve A is that calculated by Barber[6] using the valence-band data of Balslev and Lawaetz,[22] while curve B is the result of a more rigorous calculation by Madarasz *et al.*[24] using the same data. Curve C is that calculated by Humphreys[20] also using these data but a different numerical approach. Finally, curve D is that also calculated by the latter author using the different valence-band parameters attributed to Hensen.[20] The difference between curves C and D is a measure of the uncertainties arising from interpretations of the same cyclotron resonance data. None of the more recent calculations (curves B, C, and D) includes the effects of changes in the shapes of the bands with temperature. The effective mass in curve A (Ref. 6) includes multiplication by the factor $E_{G0}/E_G(T)$, where the probable origin of this factor was discussed earlier. However, theoretical studies of the temperature dependence of valence-band energies in the Brillouin zone suggest that valence bands move more or less uniformly upwards with temperature.[18,25] This would mitigate against the previous factor being appropriate. In any case, the effective-mass changes resulting from such effects of temperature upon band shape are likely to be less significant than the uncertainty apparent in Fig. 2. As previously mentioned, the latter uncertainty arises in calculating temperature dependencies resulting from anisotropy and nonparabolicity.

Prior to the present paper, there was limited experimental data for valence band effective densities-of-states effective mass at high temperature to support the previous calcu-

TABLE II. Estimates of the uncertainty in the parameters required to extract effective-mass values from the indium ionization data of Ref. 26.

Parameter	Uncertainty
Indium concentration:	
Capacitance-voltage	5%
Flameless atomic absorption	5% (Ref. 26)
Hole concentration:	
From Hall effect data	5%
Hall factor correction (Ref. 27)	5%
Indium activation energy	3 meV

lations. One source is the recent work investigating the fraction of indium dopants ionized near room temperature.[26] By comparing calculated and experimental ionization fractions, it was shown qualitatively that the effective-mass values shown in curve D of Fig. 2 gave better agreement than those of curve A or curve C. The calculational procedure outlined in Ref. 26 can be extended to give more quantitative information. By finding the precise effective-mass value to give agreement between calculated and experimental results for each of the five specimens measured, an effective-mass value of $1.10m_0$ is found at the mean sample temperature of 299 K, with a standard deviation of 10.3%. While the latter accommodates random errors in the measurement procedure, indeterminate systematic errors increase the uncertainty of this measurement approach. Using the estimates of indeterminate errors in Table II and assuming that these are independent gives the final hole density-of-states effective-mass value of $1.10(18)m_0$. The digits in parentheses in this case represent the estimate of the one-standard-deviation uncertainty in the last digits of the given mass. This experimental result is also plotted in Fig. 2, as is the low-temperature experimental cyclotron resonance result and other experimental results derived in this work, to be discussed in Sec. IV.

The above indium ionization result confirms that the valence-band effective-mass values of Barber[6] are too low near room temperature. The experimental value is in better agreement with the more recent calculations, with those by Madarasz *et al.*[24] giving the closest overall agreement. The effective mass corresponding to the latter can be described by the expression[28]

$$\frac{m^*_{dv}}{m_0} = \left(\frac{a + bT + cT^2 + dT^3 + eT^4}{1 + fT + gT^2 + hT^3 + iT^4}\right)^{2/3}, \qquad (13)$$

where the coefficients are given in Table III. Due to the good fit with the indium ionization result and the intermediate position between the two data sets calculated by Humphreys,[20] the mass given by the above equation was used in the calculations that follow.

TABLE III. Coefficients (Ref. 28) to fit the effective-mass values used in Eq. (13).

$a = 0.443\,587\,0$	$f = 0.468\,338\,2\times10^{-2}$
$b = 0.360\,952\,8\times10^{-2}$	$g = 0.228\,689\,5\times10^{-3}$
$c = 0.117\,351\,5\times10^{-3}$	$h = 0.746\,927\,1\times10^{-6}$
$d = 0.126\,321\,8\times10^{-5}$	$i = 0.172\,748\,1\times10^{-8}$
$e = 0.302\,558\,1\times10^{-8}$	

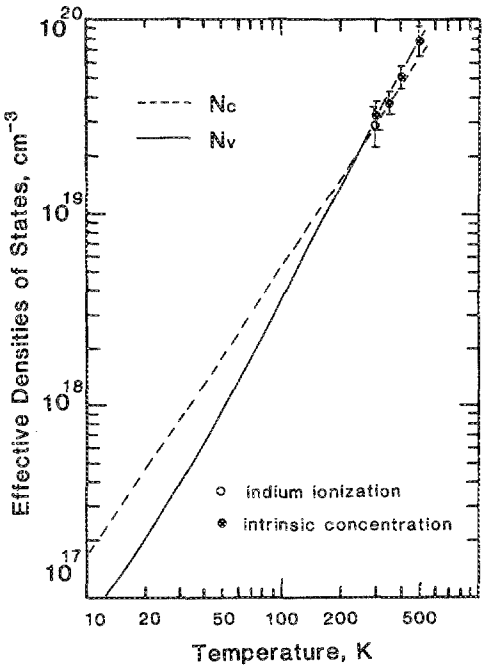

FIG. 3. Conduction- and valence-bands effective densities of states in silicon (N_C and N_V, respectively) as a function of temperature. The experimental points for N_V are derived in the present work from indium ionization data (Ref. 26) and from experimental determinations of the intrinsic carrier concentration.

Figure 3 shows the conduction- and valence-band densities of states as a function of temperature calculated using the designated effective-mass values. Note that the valence-band density of states so calculated exceeds that of the conduction band above about 250 K. Also shown is the experimentally determined value of N_V from the indium ionization results previously discussed, and other experimental results derived in Sec. IV.

At temperatures below 50 K, the temperature dependence of both calculated effective densities of states approaches the $T^{3/2}$ power expected from Eqs. (2) and (3). At higher temperatures, the temperature variation of the effective mass modifies this dependence. Over the 200–500 K temperature range, the calculated densities of states can be described to within about 2% accuracy by the expressions:

$$N_C = 2.86\times10^{19}\,(T/300)^{1.58}\ \text{cm}^{-3}, \qquad (14)$$

$$N_V = 3.10\times10^{19}\,(T/300)^{1.85}\ \text{cm}^{-3}. \qquad (15)$$

To calculate the theoretical value of the intrinsic carrier concentration, the other parameter required is the silicon band gap as a function of temperature. At the time of an earlier review by Barber,[6] the best values were those derived by Macfarlane *et al.*[19] from a careful analysis of the optical absorption edge of silicon. These had to be corrected by the exciton binding energy in silicon which, in Barber's paper,[6] was given various values in the range 0–10 meV since its value was unknown at that time.

The exciton binding energy E_{bx} has subsequently been the topic of quite extensive theoretical and experimental studies. Theoretical studies indicate the exciton ground state

is split into two energy levels [Δ_6 and Δ_7 (Ref. 29)] separated by 0.32 meV by the anisotropy of the silicon conduction bands.[30] While there is adequate experimental work supporting such a splitting,[31] the most recent experimental work suggests that each of these two levels splits further into three.[32] This is attributed to electron-hole correlation effects.[32] Five of these six levels have been identified experimentally, spread over an energy of 0.49 meV.[32]

The splitting complicates the experimental determination of E_{bx}. The most widely accepted value at present is the value of 14.7(4) meV determined from wavelength modulated optical absorption measurements.[33] The energy actually measured to produce this value is that between the ground state of the exciton and its first excited state. This is extrapolated to the value previously cited assuming a hydrogenic series of excited states. Theoretical calculations indicate that this is a reasonable assumption for excitations between "*s*-type" states.[29] The measured binding energy is assigned to the lower binding energy Δ_6 state,[29] presumably due to the strong coupling[34] between this state and the transverse optical phonon which dominates absorption processes in silicon. The measured value is in good agreement with the theoretical values[30] of 14.7 meV for the Δ_6 state and 15.0 meV for the Δ_7 state. Moreover, measured gaps between the ground state and "*p*-type" levels[32] also agree well with theory,[30] increasing confidence in a value of E_{xb} lying in the 14.7–15.0 meV range.

Since the work of Macfarlane *et al.*,[19] Bludau *et al.*[35] have reported work of a similar accuracy directed specifically at determining the variation of silicon band gap with temperature using wavelength modulation optical absorption. An error of the order of 1 meV is estimated in this work arising primarily from uncertainties in the exciton binding energy (as previously discussed), in the energy of the transverse optical phonon involved in optical absorption processes in silicon, and in the temperature dependence of both quantities.

Although Raman scattering measurements now allow a reasonably accurate estimation of the temperature variation of the TO phonon energy[36] (of the order of 0.5 meV decrease over the 0–300 K range), this was neglected in the previous work. There are no known experimental data on the temperature dependence of the exciton binding energy.

When corrected for an inappropriate conversion factor between wavelength and energy and when the exciton binding energy is added, the data of Macfarlane *et al.*[19] agree with the more recent data of Bludau *et al.*[35] to within 1 meV. Moreover, the data of Macfarlane *et al.*[19] extends to 415 K and appears to be the most accurate available beyond 300 K. Bludau *et al.*[35] have fitted their experimental data to within 0.2 meV over the range 0–190 K and 150–300 K with expressions of the form

$$E_G(T) = A + BT + CT^2, \tag{16}$$

where the coefficients A, B, and C for each of these two ranges are given in Table IV. Above 250 K, the available data can be described to within experimental accuracy (1 meV) by a simpler expression,

$$E_G(T) = 1.206 - 2.73\times10^{-4}T(\text{eV}). \tag{17}$$

TABLE IV. Coefficients for describing the variation of silicon band gap (eV) with temperature in K [$E_G(T) = A + BT + CT^2$].

T range (K)	A	B	C
0–190	1.1700	1.059×10^{-5}	-6.05×10^{-7}
150–300	1.1785	-9.025×10^{-5}	-3.05×10^{-7}
250–415	1.206	-2.73×10^{-4}	0

Given the band gap and the effective-mass values endorsed above, the value of the intrinsic carrier concentration can be calculated from Eqs. (1)–(3). Calculated values at selected temperatures are shown in Table I and will be discussed in subsequent sections. Also shown in Table I are consistent values for the thermal velocity effective masses for electrons and holes, calculated from Eq. (11) and from Ref. 20, respectively.

III. EXPERIMENTAL VALUES

A. Review of past work

The most direct measurement of the intrinsic carrier concentration involves measuring the conductivity σ of silicon at relatively high temperatures where it has intrinsic properties. At such temperatures,

$$\sigma = q(\mu_n + \mu_p)n_i, \tag{18}$$

where q is the electronic charge and μ_n and μ_p are electron and hole mobilities.

However, the mobilities are most readily measured at lower temperatures where the silicon has extrinsic properties. Hence, to determine n_i, the conductivity and the electron and hole mobilities are measured in at least two different samples over different temperature ranges.

An early but authoritative study of this type was that of Morin and Maita.[37] Intrinsic conductivity was measured at temperatures above 450 K, while mobilities were measured in the extrinsic region at 400 K and below. The mobilities, with appropriate weighting for data at the higher end of this range, were fitted by the following expressions:

$$\mu_n = \mu_{n0}\,(T/T_0)^{-\alpha_n}, \tag{19}$$

$$\mu_p = \mu_{p0}\,(T/T_0)^{-\alpha_p}, \tag{20}$$

where μ_{n0} and μ_{p0} were given the values of 1450 and 500 $\text{cm}^2\,\text{V}^{-1}\,\text{s}^{-1}$ for T_0 equal to 300 K, while α_n and α_p were assigned the values of 2.6 and 2.3, respectively.

Using these expressions to extrapolate mobilities to the higher-temperature intrinsic regions allows the intrinsic concentration to be found. The expression fitted to the data so calculated takes the following form below 700 K[37]:

$$n_i = 3.87\times10^{16}T^{3/2}\exp(-0.605q/kT)\ \text{cm}^{-3}. \tag{21}$$

Putley and Mitchell[38] undertook similar measurements but used much more lightly doped specimens which extended the intrinsic region of operation to below 400 K. Conductivity mobility was not measured in this work but was calculated from the measured Hall mobility. To counteract possible limitations of this procedure, the intrinsic concentration was also calculated using the minority-carrier drift

mobility measurements of Ludwig and Watters.[39] The final expression for the intrinsic carrier concentration derived by Putley and Mitchell[38] gave approximately equal weight to values of n_i derived using both types of mobility data and took the form

$$n_i = 3.10\times10^{16}T^{3/2}\exp(-0.603q/kT)\ \text{cm}^{-3}. \quad (22)$$

Wasserrab[40] combined the more comprehensive conductivity measurements of Fulkerson *et al.*[41] with the mobility data accumulated by Jacoboni *et al.*[42] giving the following expression for n_i:

$$n_i = 5.71\times10^{19}(T/300)^{2.365}\exp(-6733/T)\ \text{cm}^{-3}. \quad (23)$$

A significant contribution to this area overlooked in previous reviews[6,40,43] is work on "superpure" float-zone silicon subject to 71 zone passes by Hoffmann *et al.*[44] This material had a room-temperature resistivity of 150 K Ω cm compared to the 6 K Ω cm material[38] which was the purest material used in previous studies. This material entered the intrinsic range at relatively low temperatures above 310 K. Measurement of the conductivity up to 373 K allowed intrinsic concentrations to be calculated at much lower temperatures than previous measurements. Calculated values were in good agreement with values given by Eq. (22) from the work of Putley and Mitchell,[38] although slightly lower at the lowest temperatures involved.

Finally, Herlet[45] calculated the temperature dependence of n_i from the temperature dependence of *p-i-n* junction diode characteristics. This approach has the advantage of extending measurements to lower temperature. It, however, requires a knowledge of the temperature dependence of additional semiconductor parameters. It is consequently not as direct an approach as that based on the intrinsic conductivity. Results derived are inconsistent with those of Hoffmann *et al.*[44]

B. Reassessment of experimental n_i

1. Intrinsic resistivity

Above 500 K, there have been several studies of the resistivity of intrinsic silicon.[37,41,46] All these give virtually identical results. They show an intrinsic resistivity (ρ_i) whose logarithm increases linearly with increasing $1/T$

$$\log(\rho_i) = A + B/T. \quad (24)$$

Values of the intrinsic resistivity extracted from the published curves resulting from the previous studies all agree to the accuracy with which data can be extracted.

Of these, the work of Fulkerson *et al.*[41] was chosen as being the most suitable for the present purposes. One advantage is that a relatively high extrinsic resistivity sample was used in this study (150 Ω cm at room temperature) which extends the intrinsic region to below 500 K. A second advantage was a relatively large number of data points in the intrinsic range of operation. A third advantage is the inclusion of error estimates. The accuracy of the resistivity measurement is estimated as 1.8% while the accuracy of temperature measurement was conservatively estimated as 2 °C.

These authors used both polycrystalline and single-crystalline samples in their study and arrived at values in Eq. (24) of $A = -4.247$ and $B = 2.924$, for T in K and ρ_i in Ω cm. Unfortunately, the accuracy of the fit of this expression to the experimental data was not discussed. The authors state that results for polycrystalline and crystalline specimens agreed to about 2%. However, the above values of A and B do not give agreement to this accuracy with the results shown by these authors in graphical form for a single-crystal specimen subject to quite extensive measurement. Since single-crystal silicon was of prime interest in the present work, the published data for single-crystal silicon was refitted giving $A = -4.2953$ and $B = 2947.8$. These values are only about 1% different from those published by Fulkerson *et al.*[41]

Values calculated with these revised values are shown in the top row of Table V. The values above 500 K agree with the published data of Fulkerson *et al.*[41] for single-crystal silicon, while also giving very good agreement with those of Morin and Maita[31] and Burton and Madjid[46] at temperatures where intrinsic behavior is displayed.

Below 500 K, there are less extensive data available due to the high resistivities required to maintain intrinsic properties at such temperatures. Putley and Mitchell[38] have measured the intrinsic conductivity at temperatures below 400 K using specimens of room-temperature extrinsic resistivity in the 2–6 kΩ cm range. Their results highlight the need to apply corrections to the measured data once the intrinsic resistivity reaches a value within about an order of magnitude of the extrinsic resistivity. Putley and Mitchell[38] show data for three specimens with about 30% difference between intrinsic resistivity values around 500 K. However, for un-

TABLE V. Experimental values of the intrinsic resistivity of silicon (ρ_i) as a function of absolute temperature (T). The digits in parentheses are estimates of the one-standard-deviation uncertainty in the last digits of the given resistivity. The values shown are based on fitting the equation $\log(\rho_i) = A + B/T$ to the experimental data. The coefficients A and B are shown for the three data sets tabulated, for T in K and ρ_i in Ω cm.

	Resistivity (kΩ cm)						Coefficients	
Reference	$T = 300$ K	$T = 350$ K	$T = 400$ K	$T = 500$ K	$T = 700$ K	$T = 1000$ J	A	B
41	339(71)k[a]	13.40(210)k[a]	1186(140)[a]	39.8(8)	0.824(16)	0.0449(9)	−4.2953	2947.8
38	303(48)k[a]	12.46(121)k[a]	1138(34)	39.9(12)			−4.2187	2910.0
44	292(29)k[a]	13.15(79)k	1286(144)[a]				−3.9605	2827.8
Assigned value	300(23)k	12.98(63)k	1148(32)	40(1)	0.82(2)	0.045(1)	···	···

[a] Extrapolated value ($k \equiv$ K Ω cm).

specified reasons, these authors express most confidence in one sample (ZG131) for which an accuracy of 5% is estimated. This sample gives excellent agreement with the subsequent results of Fulkerson *et al.*[41] around 500 K as indicated in Fig. 4. After correcting the data at lower temperature to account for the onset of the transition from intrinsic to extrinsic behavior, the results for this specimen could be very accurately fitted by Eq. (24) with $A = -4.2187$ and $B = 2910.0$. The corresponding values of the intrinsic resistivity are shown as the second row in Table V.

The only known data extending these measurements to lower temperatures are those of Hoffmann *et al.*[44] The specimens used in this work were subject to up to 71 zone passes giving room-temperature resistivities as high as 150 kΩ cm. The intrinsic region of operation correspondingly extended to temperatures as low as 40 °C. The intrinsic resistivity was measured up to 100 °C using a water bath for temperature control. The small temperature range of these measurements and the scatter observed in the experimental data (possibly due to the increased sensitivity to inaccuracies in temperature measurement) combine to limit the utility of these data (third row of Table V). However, as seen in Fig. 4, these data provide a consistent extension of the higher-temperature data of Burton and Madjid,[46] Fulkerson *et al.*,[41] and Putley and Mitchell[38] to lower temperatures.

The uncertainty estimates of Table V are based on the assessed measurement accuracy at temperatures where extrapolation of Eq. (24) outside the measurement region is not required. When extrapolation is required, there is increased uncertainty for two reasons. One reason is purely statistical in that uncertainties in the slope of A will lead to increasing uncertainties in estimating ρ_i as $1/T$ moves away from the central region of the measurement range.[47] The second is that there is no guarantee, even with a perfect fit to the data over the measurement range, that the fitted curve would hold outside this range.[47] Both types of uncertainties are included in the uncertainty estimates of Table V. To accommodate the latter uncertainty, an additional uncertainty of $10\,000\Delta(1/T)\%$ in the value of $\log(\rho_i)$ was included in all extrapolated data. $\Delta(1/T)$ is the difference between the reciprocal temperature at the extrapolated point and at the central region of the measurement range. This uncertainty estimate was based on considering the balance between the temperature dependency of the terms in Eqs. (1) and (18) required for Eq. (24) to accurately describe the observed resistivity dependence.

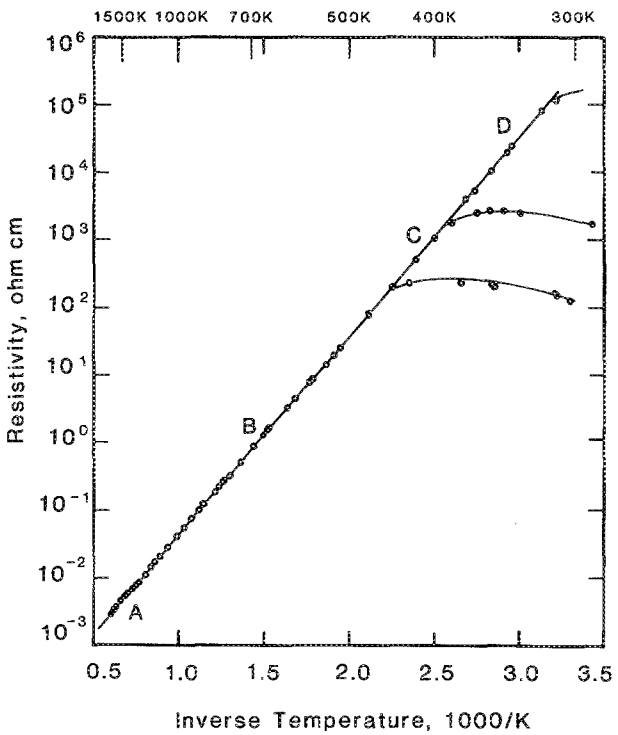

FIG. 4. The resistivity of silicon as measured by several groups as a function of inverse temperature for temperatures between the melting point of silicon and room temperature. The transition from the intrinsic region (approximately linear curve) to the extrinsic region is shown for three of the data sets. Region A shows data from Ref. 46, B from Ref. 41, C from Ref. 38, and D from Ref. 44.

The best estimates of the intrinsic resistivity at each temperature were then found by finding an optimally weighted average of the values given in Table V from the three data sets. At temperatures above 400 K, the one-standard-deviation uncertainty in the value so extracted is only a few percent. However, this uncertainty increases rapidly at lower temperature towards a value of 10%. This is due to the increasing uncertainty in the data of Fulkerson *et al.*[41] due to the additional extrapolation penalty previously described. In the case of the data of Putley and Mitchell,[38] the relatively small measurement range also contributes a significant statistical component to the extrapolated uncertainty. In the case of the data of Hoffmann *et al.*,[44] the scatter in the experimental data itself is the most significant source of uncertainty. Additional low-temperature data using high resistivity silicon would help reduce the overall uncertainty at such temperatures.

Note that there is some experimental support for a decrease in the slope coefficient B as the temperature decreases with a correlated decrease in the magnitude of coefficient A (the ratio $-B/A$ gives the temperature where the intrinsic resistivity, or its extrapolated value, would equal 1 Ω cm).

2. Mobility

There have been several studies of the electron and hole mobilities in pure silicon near 300 K.[17,39,42,48–55] These place the electron mobility in the range 1350–1500 $cm^2\ V^{-1}\ s^{-1}$ and the hole mobility in the range 450–510 $cm^2\ V^{-1}\ s^{-1}$ at 300 K. In the most comprehensive recent study conducted by the National Bureau of Standards in Washington, DC, values of 1415 and 471 $cm^2\ V^{-1}\ s^{-1}$, respectively, are determined for lightly doped specimens with an estimated total error of 5% and 3%, respectively.[54]

For the electron mobility, the sources of the lowest-lying values are Refs. 39 and 50. In the case of Ref. 50, there is a very large scatter in the reported data which would result in very little weight being given to these measurements. In the case of Ref. 39, the experimental results divide into two groups with different low-temperature behavior at temperatures below 200 K. This suggests either significant compensation or the presence of substantial concentrations of neutral impurities for the group with lower mobility at low temperature. Neglecting the results for these specimens on

this account gives an average mobility for the remaining data of 1417 $cm^2 V^{-1} s^{-1}$ (range 1400–1430 $cm^2 V^{-1} s^{-1}$), in excellent agreement with the results of Thurber *et al.*[54] The source of the highest-lying electron mobility value is Ref. 48 based on extrapolating values measured on relatively highly doped specimens. Subsequently, Zerbst and Heywang[49] extended these measurements to include more lightly doped specimens. This produced good agreement in overlapping substrate resistivity ranges but gave a more accurate extrapolated value in the 1400–1450 $cm^2 V^{-1} s^{-1}$ range, again in good agreement with the results of Thurber *et al.*[54]

Hence, no strong case could be found for electron mobility values substantially different from those of Thurber *et al.*[54] The results of Zerbst and Heywang,[49] however, do provide some support for a slight increase in mobility for lower doping levels than the value of 2.7×10^{13} cm^{-3}, which was the lowest doping level used by Thurber *et al.*[54] Hence, a slightly increased value of 1430(46) $cm^2 V^{-1} s^{-1}$ was assigned to the 300-K electron mobility in this work. The one-standard-deviation uncertainty in this mobility shown in parentheses was estimated using a technique employed in estimating uncertainties in the recommended values of the physical constants.[5] A semirange a of 80 $cm^2 V^{-1} s^{-1}$ was assigned to the maximum likely error in the mobility value due primarily to "type-B" errors (those not amenable to evaluation by statistical techniques). The equivalent variance was then taken to be $a^2/3$.

For the hole mobility, the sources of the more extreme values are again Refs. 39 and 50. Similar arguments apply in this case. The combined results of Refs. 50 and 49 extrapolate to a value in the 470–500 $cm^2 V^{-1} s^{-1}$ range. The data of Ludwig and Watters[39] divide into three groups based on temperature dependence. The group with the highest mobility at low temperatures (100 K) give a mobility of 475 $cm^2 V^{-1} s^{-1}$ at 300 K, again in excellent agreement with the results of Thurber *et al.*[54] For similar reasons, as for the case of the electron mobility, a slightly higher hole mobility of 480(17) $cm^2 V^{-1} s^{-1}$ is used in this work (semirange a of 30 $cm^2 V^{-1} s^{-1}$).

To calculate the experimental intrinsic conductivity using Eq. (18), the sum of electron and hole mobilities is required. A value of 1910(49) $cm^2 V^{-1} s^{-1}$ is deduced assuming independence of the electron and hole mobility uncertainties.

Although there is a reasonable amount of data available for carrier mobilities below 300 K, there are surprisingly limited primary data for temperatures above 300 K. The most useful way of characterizing these data is by fitting to a power law as in Eqs. (19) and (20) over the temperature range of interest. The results so derived for the power terms, α_n and α_p, are given in Table VI.

These results are listed with those rated most reliable listed first. A high rating is given to the drift mobility results of Ludwig and Watters[39] for their highest low-temperature mobility specimens on several accounts. They give good agreement with the 300-K mobility values deduced by Thurber *et al.*[54] The results also involve measurements on several samples over a wide temperature range. A somewhat lower rating is given to the coefficients deduced by these authors from conductivity measurements since an assumption is involved about the constancy of the majority-carrier concentration with temperature. In the case of drift measurements, minority-carrier mobilities are measured while conductivity measurements give majority carrier mobilities. However, no differences on this account are expected for the lightly doped specimens involved.

The next highest weight is given to values of α_n deduced from the normalized room-temperature coefficients of resistivity measured by Bullis *et al.*[56] From Eqs. (19) and (20), it is simply shown that multiplying this resistivity coefficient by the temperature at which it is measured gives the required mobility coefficient at this temperature, assuming temperature independence of majority-carrier concentrations. Good consistency is obtained in these data[56] as substrate doping varies with small experimental uncertainties in the values deduced. A somewhat lower rating is given to the values of α_p so deduced, mainly due to scatter seen in the data for the lowest doped specimens. Both α_n and α_p are in close agree-

TABLE VI. Temperature dependence of electron and hole mobilities μ_n and μ_p in silicon. Shown are the values of the power terms, α_n and α_p, in the expression $m = \mu_0(T/T_0)^{-\alpha}$ for different temperature ranges as deduced from previous experimental and theoretical work.

	α_n			α_p		
Technique	200–300 K	300–400 K	400–500 K	200–300 K	300–400 K	400–500 K
Experiment						
Drift (Ref. 39)	2.5	2.5	···	2.7	2.7	···
Conductivity (Ref. 39)	2.5	2.5	···	2.7	2.7	···
T Coefficient (Ref. 56)	2.44(5)[a]	2.44(5)[a]	···	2.5–2.8[a]	2.5–2.8[a]	
Conductivity (Ref. 57)	2.3	2.3		2.3–2.4	2.3–2.4	
Conductivity (Ref. 37)	···	2.6	···	2.3	2.3	···
Drift (Ref. 49)	2.3	2.3	···	2.3	2.3	···
Time of Flight (Ref. 51)	···	···	···	2.6	···	···
Compilation (Ref. 42)	2.42	···	···	2.20	···	···
Theoretical						
Model III (Ref. 17)	2.4	2.3	2.0	···	···	···
Deformation potential (Ref. 55)	···	···	···	2.5	2.3	2.1
Assigned value	2.5(2)	2.5(2)	2.4(4)	2.5(3)	2.5(3)	2.4(3)

[a] At 296 K only.

TABLE VII. Experimental electron and hole mobilities of pure silicon (μ_n and μ_p) and their sum as a function of temperature. The values shown are derived from the 300-K value of mobility and the temperature power coefficients given in Table VI. The digits in parentheses are the calculated one-standard-deviation uncertainty in the last digits of the given mobility, based on the corresponding uncertainty estimates for the 300-K mobility and those for the coefficients (Table VI).

Mobility	200 K	300 K	350 K	400 K	500 K
μ_n ($cm^2 V^{-1} s^{-1}$)	3941(379)	1430(46)	973(44)	697(47)	408(39)
μ_p ($cm^2 V^{-1} s^{-1}$)	1323(178)	480(17)	326(19)	234(23)	137(23)
$\mu_n + \mu_p$	5263(419)	1910(49)	1299(48)	930(52)	545(43)

ment with the values of Ludwig and Watters[39] previously discussed.

A high weight is also given to the α_p values deduced by Evans[57] from conductivity measurements upon six high resistivity p-type specimens. These gave somewhat lower values of α_p consistently in the 2.3–2.4 range. A lower weight is given to the corresponding value of α_n due to the experimental difficulties experienced with n-type samples.[57]

The next highest weight is given to the hole mobility coefficients deduced from conductivity measurements by Morin and Maita.[37] A somewhat lower weight is given to the electron mobility coefficient similarly deduced by these authors due to the incompletely described corrections applied for ionized impurity scattering in this case. A lower rating is given to the drift results of Zerbst and Heywang[49] due to the low room-temperature mobility of the samples used in their temperature studies. This will tend to give lower values of these coefficients than higher mobility samples. The time-of-flight measurements of Ottaviani *et al.*[51] are given a lower rating due to the scatter in the corresponding coefficient seen at lower temperatures in values deduced by this technique. Finally, the values deduced by Jacoboni *et al.*[42] are given a low rating due to their dependence on Hall effect data and the associated uncertainties in Hall factor as a function of temperature.

The theoretical results shown indicate a trend to lower values of the coefficients as temperature increases. Some weight has been given to these predictions in assigning values to the coefficients over the 400–500 range, where there are virtually no experimental data. Note, however, that some doubt is cast on the theory by its inability, in the case of Norton *et al.*,[17] to describe the measured Hall factor variation above room temperature. In the case of the hole mobility, Szmulowicz[55] mentions the possibility that this reduction in the coefficient at high temperature may result from inadequacies of the 6×6 **k·p** Hamiltonian used in the calculations.

Using the room-temperature mobility values previously discussed and the assigned values of these temperature coefficients gives the best experimentally based estimates of the electron and hole mobilities of pure silicon as a function of temperature as shown in Table VII.

3. Experimental intrinsic concentration

Using Eq. (18), the experimental value of the intrinsic concentration can be derived from the experimental intrinsic resistivity values of Table V and the mobility values of Table VII. The resulting experimental values are included in Table VIII.

As can be deduced from the uncertainties shown, best experimental accuracy is obtained in the 350–400 K range. Uncertainties in the intrinsic resistivity at lower temperatures and in the carrier mobilities at higher temperatures result in poorer accuracy outside this range.

IV. COMPARISON BETWEEN CALCULATED AND EXPERIMENTAL RESULTS

Shown in Table VIII are the experimental values of the intrinsic carrier concentration of the previous section together with the calculated values of Sec. II over the temperature range of interest. Also shown are the values deduced from the three equations for n_i described in the text.

The calculated values have also been assigned a one-standard-deviation uncertainty based on the uncertainties in effective masses and band gap estimated in Table IX. The largest uncertainty is associated with the valence-band effective mass due to the variation in its calculated value depending on the interpretation of low-temperature cyclotron resonance data and the calculational procedure employed (see

TABLE VIII. Comparison between experimentally determined and calculated values of the intrinsic carrier concentration in silicon as a function of temperature. Also shown are the values given by three equations suggested in earlier work. The digits in parentheses are estimates of the one-standard-deviation uncertainty in the last digits of the corresponding concentrations.

T (K)	Units (cm^{-3})	Experiment	Calculated	Eq. (23)	Eq. (22)	Eq. (21)
200	10^4		5.03(59)	5.24	5.60	6.24
300	10^{10}	1.09(9)	1.07(12)	1.02	1.19	1.38
350	10^{11}	3.70(22)	3.92(46)	3.63	4.21	4.92
400	10^{12}	5.85(37)	6.00(72)	5.52	6.27	7.40
500	10^{14}	2.86(24)	2.89(35)	2.71	2.90	3.46

TABLE IX. Assigned uncertainties for estimates of calculated silicon intrinsic concentration accuracy.

Parameter		200 K	300 K	350 K	400 K	500 K
Effective masses:	m_l^*	1%	2%	2.5%	3%	5%
	m_t^*	1%	2%	2.5%	3%	5%
	m_{dv}^*	15%	15%	15%	15%	15%
Band gap:	E_g	1 meV	1.5 meV	2 meV	2.5 meV	3 meV

Fig. 2 and associated discussion). Uncertainty in the value of the band gap is a smaller contributor. Below 200 K, this contribution would become more severe.

Good agreement is observed between the experimental and calculated intrinsic concentrations over the temperature range where a comparison is meaningful. Since these two values are deduced from completely independent arguments, there is sufficient information available to provide new estimates of any one of the material parameters appearing in Eq. (1) [or its subsidiary equations (2) and (3)] or in Eq. (18). This can be achieved by equating Eqs. (1) and (18) and treating the parameter of interest as unknown.

Since the largest uncertainties arise in the hole density-of-states effective mass value, m_{dv}^*, this procedure produces the most useful information in this case. Figure 2 includes the values deduced for this parameter in this way. These results are in best agreement with the calculations of Madarasz *et al.*[24] although those of Humphreys[20] using the Hensel valence-band parameters are also in reasonable agreement. The calculated results of Barber[6] lie approximately two standard deviations below the experimentally determined values.

Figure 3 shows the corresponding experimentally determined effective density of states in the valence band, in good agreement with those previously calculated. Note that the value of this parameter of $3.1(5)\times10^{19}$ cm^{-3} at 300 K, deduced from the two independent experimental measurements at this temperature, is well in excess of a commonly cited value of 1.04×10^{19} cm^{-3} (Refs. 1, 3, and 4) and higher than the value of 1.85×10^{19} cm^{-3} deduced from the work of Barber.[6] This significantly higher value will impact most calculations of energy with respect to the valence-band edge in silicon. Errors of up to 30 meV could arise in such cases, near room temperature, by using less appropriate values.[1,3,4,6]

Also shown in Table VIII are the values of the intrinsic concentration at the temperatures shown calculated from the expressions derived from earlier studies [Eqs. (21)–(23)]. Note that the results deduced by Wasserab [Eq. (23)] lie within one standard deviation of both the present experimental and calculated values. Those of Putley and Mitchell [Eq. (22)] are further removed from the present experimental values but lie within one standard deviation of the present calculated values. However, those of Morin and Maita [Eq. (21)] lie well beyond one standard deviation of the present calculated values and are even further removed from the present experimental values.

By forming a weighted average of the present independent experimental and theoretical estimates, a value of the intrinsic carrier concentration of $1.08(8)\times10^{10}$ cm^{-3} at 300 K is deduced. The commonly used value at present of 1.45×10^{10} cm^{-3} at 300 K (Refs. 1, 3, and 4) is many standard deviations removed from this value and is higher than that given by any previous study apart from that of Herlet.[45] The latter was previously discounted (Sec. III A) due to the additional uncertainties involved in the corresponding measurement approach.

The origin of the value of 1.45×10^{10} cm^{-3} at 300 K is uncertain. One possibility is that it arises from rounding of the value of the exponent in the expression of Morin and Maita.[37] Wasserrab[40] shows that this explains the value of 1.5×10^{10} cm^{-3} calculated by Conwell.[58] Evaluating the latter expression using a value of kT of 25.9 meV rather than the value of 25.85216(22) meV derived from presently recommended values of the physical constants[5] gives $n_i = 1.44\times10^{10}$ cm^{-3}. Another possible origin of this figure might be as the arithmetic mean of the value of 1.5×10^{10} cm^{-3} calculated by Conwell[58] and the value of 1.4×10^{10} cm^{-3} which results from the correct evaluation of the expression given by Morin and Maita.[37]

Regardless of the origin of the figure of 1.45×10^{10} cm^{-3}, it is not supported by either the best available experimental data or by theory. Since current flows in bipolar semiconductor devices generally depend on n_i^2, use of this value will overestimate current flows at a fixed voltage in such devices by a factor approaching 2. Conversely, the applied voltage required to pass a given current will be underestimated by about 15 mV near room temperature.

V. CONCLUSION

The source of an inconsistency between commonly used values of the silicon intrinsic concentration, the conduction- and valence-band effective densities of states, and the band gap has been investigated.

By incorporating recent data for the hole "densities-of-states" effective mass and by critically reevaluating earlier intrinsic carrier concentration measurements, this discrepancy is eliminated. One significant result of this re-assessment is that the commonly used value of 1.45×10^{10} cm^{-3} for the silicon intrinsic concentration at 300 K (Refs. 1, 3, and 4) is not supported by the best available experimental data nor by theory. A preferred value deduced in the present work is $1.08(8)\times10^{10}$ cm^{-3} where the digit in parentheses represents the estimated one-standard-deviation uncertainty

in the last digit of the previous value. This difference is particularly significant in silicon device analysis where an overestimate of current flows at a given applied voltage by a factor approaching 2 could be calculated using the larger value.

A second significant result is the determination of experimentally based values of the hole "densities-of-states" effective mass in silicon at temperatures in the 300–500 K range by two independent techniques. These experimental results are in good agreement with the theoretical calculations of Humphreys[20] and Madarasz *et al.*[24] At 300 K, an experimental valence-band effective densities of states of $3.1(5)\times10^{19}$ cm^{-3} is determined from these effective mass values. This is appreciably higher than the commonly cited values of 1.04×10^{19} cm^{-3} (Refs. 1, 3, and 4) and 1.85×10^{19} cm^{-3} (Ref. 6). This significantly higher revised value, for which there is also theoretical support,[20,24] will impact calculations of energies with respect to the valence-band edge in silicon. Differences of up to 30 meV may arise near room temperature.

ACKNOWLEDGMENTS

Support of related work by the Australian Research Council and by Sandia National Laboratories is gratefully acknowledged. The Joint Microelectronics Research Centre is supported by the Commonwealth Special Research Centres Scheme.

[1]S. M. Sze, *Physics of Semiconductor Devices*, 2nd ed. (Wiley, New York, 1981).
[2]A. G. Milnes, *Deep Impurities in Semiconductors* (Wiley, New York, 1973).
[3]H. F. Wolf, *Semiconductors* (Wiley, New York, 1971).
[4]O. D. Trapp, R. A. Blanchard, and W. H. Shepperd, *Semiconductor Technology Handbook* (Technology Associates, Portola Valley, 1980); W. C. O'Mara, in *Semiconductor Materials and Process Technology Handbook*, edited by G. E. McGuire (Noyes, Park Ridge, 1988).
[5]E. R. Cohen and B. N. Taylor, Codata Bull. **63**, 1 (1986).
[6]H. D. Barber, Solid-State Electron. **10**, 1039 (1967).
[7]T. Nishino, M. Takeda, and Y. Hamakawa, Solid State Commun. **14**, 627 (1974).
[8]J. C. Hensel, H. Hasegawa, and M. Nakayama, Phys. Rev. **138**, A225 (1965).
[9]For example, W. A. Harrison, *Solid State Theory* (McGraw-Hill, New York, 1970); A. Van der Ziel, *Solid State Physical Electronics* (Prentice-Hall, NJ, 1976).
[10]G. Dresselhaus, A. F. Kip, and C. Kittel, Phys. Rev. **98**, 368 (1955).
[11]R. N. Dexter, H. J. Zeiger, and B. Lax, Phys. Rev. **104**, 637 (1956).
[12]G. J. Rauch, J. J. Stickler, G. S. Heller, and H. J. Zeiger, Phys. Rev. Lett. **4**, 64 (1960).
[13]D. M. S. Bagguley, R. A. Stradling, and J. J. Whiting, Proc. R. Soc. London Ser. A **262**, 365 (1961).
[14]R. A. Stradling and V. V. Zhukov, Proc. Phys. Soc. London **87**, 263 (1966).
[15]Yu. I. Ukhanov and Yu. V. Mal'tsev, Sov. Phys. Solid State **5**, 2144 (1964).
[16]J. C. Ousset, J. Leotin, S. Askenazy, M. S. Skolnick, and R. A. Stradling, J. Phys. C **9**, 2803 (1976).
[17]P. Norton, T. Braggins, and H. Levinstein, Phys. Rev. B **8**, 5632 (1973).
[18]P. Lautenschlager, P. B. Allen, and M. Cardona, Phys. Rev. B **31**, 2163 (1985).
[19]G. G. Macfarlane, T. P. McClean, J. E. Quarrington, and V. Roberts, Phys. Rev. **111**, 1245 (1958).
[20]R. G. Humphreys, J. Phys. C **14**, 2935 (1981).
[21]J. C. Hensel and G. Feher, Phys. Rev. **129**, 1041 (1963).
[22]I. Balslev and P. Lawaetz, Phys. Lett. **19**, 6 (1965).
[23]P. Lawaetz, Phys. Rev. B **4**, 3460 (1971).
[24]F. L. Madarasz, J. E. Lang, and P. M. Hemeger, J. Appl. Phys. **52**, 4646 (1981).
[25]D. Auvergne, J. Camassel, H. Mathieu, and M. Cardona, Phys. Rev. B **9**, 5168 (1974).
[26]G. J. Parker, S. D. Brotherton, I. Gale, and A. Gill, J. Appl. Phys. **54**, 3926 (1983).
[27]J. F. Lin, S. S. Li, L. C. Linares, and K. W. Teng, Solid-State Electron. **24**, 827 (1981).
[28]J. E. Lang, F. L. Madarasz, and P. M. Hemeger, J. Appl. Phys. **54**, 3612 (1983).
[29]N. O. Lipari and M. Altarelli, Phys. Rev. B **15**, 4883 (1977).
[30]N. O. Lipari and M. Altarelli, Solid State Commun. **32**, 171 (1979).
[31]M. L. W. Thewalt and W. G. McMullan, Phys. Rev. B **30**, 6232 (1984).
[32]D. Labrie, M. L. W. Thewalt, I. J. Booth, and G. Kirczenow, Phys. Rev. Lett. **61**, 1882 (1988).
[33]K. L. Shaklee and R. E. Nahory, Phys. Rev. Lett. **24**, 942 (1970).
[34]D. L. Smith, N. R. B. Hammond, M. Chen, S. A. Lyon, and T. C. McGill, in *Proceedings of the XIII International Conference on the Physics of Semiconductors*, Rome, 1976 (North-Holland, Amsterdam, 1976), p. 1077; R. B. Hammond and R. N. Silver, Solid State Commun. **28**, 993 (1978).
[35]W. Bludau, A. Onton, and W. Heinke, J. Appl. Phys. **45**, 1846 (1974).
[36]R. Tsu and J. G. Hernandez, Appl. Phys. Lett. **41**, 1016 (1982); M. Balkanski, R. F. Wallis, and E. Haro, Phys. Rev. B **28**, 1928 (1983).
[37]F. J. Morin and J. P. Maita, Phys. Rev. **96**, 28 (1954).
[38]E. H. Putley and W. H. Mitchell, Proc. Phys. Soc. **72**, 193 (1958).
[39]G. W. Ludwig and R. L. Watters, Phys. Rev. **101**, 1699 (1956).
[40]Th. Wasserrab, Z. Naturforsch. **32a**, 746 (1977).
[41]W. Fulkerson, J. P. Moore, R. K. Williams, R. S. Graves, and D. L. McElroy, Phys. Rev. **167**, 765 (1968).
[42]C. Jacoboni, C. Canali, G. Ottaviani, and A. A. Quaranta, Solid-State Electron. **20**, 77 (1977).
[43]G. Gagliana and L. Reggiani, Il Nuovo Cimento **30B**, 207 (1975).
[44]A. Hoffmann, K. Reuschel, and H. Rupprecht, J. Phys. Chem. Solids **11**, 284 (1959).
[45]A. Herlet, Z. Angew. Phys. **9**, 155 (1957).
[46]L. C. Burton and A. H. Madjid, Phys. Rev. **185**, 1127 (1969).
[47]T. H. Wonnacott and R. J. Wonnacott, *Regression: A Second Course in Statistics* (Wiley, New York, 1981), p. 49.
[48]M. B. Prince, Phys. Rev. **93**, 1204 (1954).
[49]M. Zerbst and W. Heywang, Z. Naturf. **11a**, 608 (1956).
[50]D. C. Gronemeyer, Phys. Rev. **105**, 522 (1957).
[51]G. Ottaviani, L. Reggiani, C. Canali, F. Nava, and A. A. Quaranta, Phys. Rev. B **12**, 3318 (1975).
[52]S. S. Li and W. R. Thurber, Solid-State Electron. **20**, 609 (1977).
[53]S. S. Li, Solid-State Electron. **21**, 1109 (1978).
[54]W. R. Thurber, R. L. Mattis, and Y. M. Liu, *The Relationship Between Resistivity and Dopant Density for Phosphorus- and Boron-Doped Silicon*, National Bureau of Standards, Special Publication 400-64 (U.S. GPO, Washington, DC, 1981).
[55]F. Szmulowicz, Phys. Rev. B **28**, 5943 (1983).
[56]W. M. Bullis, F. H. Brewer, C. D. Kolstad, and L. J. Swartzendruber, Solid-State Electron. **2**, 639 (1968).
[57]D. M. Evans, J. Electron. Control **1**, 112 (1959).
[58]E. M. Conwell, Proc. IRE **46**, 1281 (1958).